

# A Glyph-driven Topology Enhancement Network for Scene Text Recognition

1<sup>st</sup> Tongkun Guan

*Department of Automation  
Shanghai Jiao Tong University  
Shanghai, China  
gtk0615@sjtu.edu.cn*

2<sup>nd</sup> Chaochen Gu

*Department of Automation  
Shanghai Jiao Tong University  
Shanghai, China  
jacygu@sjtu.edu.cn*

3<sup>rd</sup> Jingzheng Tu

*Department of Automation  
Shanghai Jiao Tong University  
Shanghai, China  
tujingzheng@sjtu.edu.cn*

4<sup>th</sup> Xue Yang

*Department of Computer Science and Engineering  
Shanghai Jiao Tong University  
Shanghai, China  
yangxue-2019-sjtu@sjtu.edu.cn*

5<sup>th</sup> Qi Feng

*Department of Automation  
Shanghai Jiao Tong University  
Shanghai, China  
fengqi@sjtu.edu.cn*

**Abstract**—Attention-based methods by establishing one-dimensional (1D) and two-dimensional (2D) mechanisms with an encoder-decoder framework have dominated scene text recognition (STR) tasks due to their capabilities of building implicit language representations. However, 1D attention-based mechanisms suffer from alignment drift on latter characters. 2D attention-based mechanisms only roughly focus on the spatial regions of characters without excavating detailed topological structures, which reduces the visual performance. To mitigate the above issues, we propose a novel Glyph-driven Topology Enhancement Network (GTEN) to improve topological features representations in visual models for STR. Specifically, an unsupervised method is first employed to exploit 1D sequence-aligned attention weights. Second, we construct a supervised segmentation module to capture 2D ordered and pixel-wise topological information of glyphs without extra character-level annotations. Third, these resulting outputs fuse enhanced topological features to enrich semantic feature representations for STR. Experiments demonstrate that GTEN achieves competitive performance on IIIT5K-Words, Street View Text, ICDAR-series, SVT Perspective, and CUTE80 datasets.

**Index Terms**—Scene text recognition, Attention mechanism

## I. INTRODUCTION

Scene text recognition (STR) aims to recognize regular and irregular texts from multi-scene images, which is widely applied in handwriting recognition [46], industrial print recognition [13], and visual understanding [8]. Apart from the indefinite-length character sequence problem of the off-the-shelf optical character recognition (OCR) in documents, the STR task is challenged by irregular structures (*i.e.*, curved, oriented, and distorted texts), low resolution, heavy occlusion, and uneven illumination.

Inspired by natural language processing methods, the encoder-decoder architectures with attention mechanisms are developed to solve the aforementioned challenges [3], [23], [49], [50]. The encoder extracts visual features of text images and outputs semantic feature representations, and the decoder builds attention mechanisms to capture time-dependently at-

tentional character features at different decoding steps. These attention mechanisms are summarized into one-dimensional (1D) attention and two-dimensional (2D) attention mechanisms.

Specifically, the encoder-decoder methods [7], [9], [25], [26], [37]–[39] with 1D attention mechanism employ long short-term memory (LSTM) [16] units to build implicit language representations with attentive feature sequences, and then output character classes sequentially. As briefly shown in Fig. 1(a), each row represents the visualization result of attention weight generated by the TRBA model [3] at different decoding steps. The attention weight, which focuses on the important items of the encoder outputs, is multiplied by the encoder outputs to generate a *glimpse* feature vector for character recognition. Although these 1D attention-based methods fastly and robustly recognize regular texts, they perform ineffectively on irregular and long texts due to the alignment-drifted sequential attention. In contrast, 2D attention-based methods [11], [22], [23], [46], [49] propose various 2D attentional feature representations by embedding time-dependent sequences into the whole network to capture spatial features of corresponding characters at different decoding steps, as shown in Fig. 1(b). Some segmentation-based works [24], [29] design character segmentation networks supervised by extra character-level annotations for text recognition without considering the large workload and difficulty of annotations in public real-world datasets. Although these 2D attention-based methods provide an effective solution to recognize irregular texts, the extracted 2D attentional features focus on spatial regions of characters and less consider the topological information of glyphs (e.g., contour and pixel-level location), leading to performance degradation. The topological information of glyphs enhances the discrimination of different characters in the middle neural network layer, which is fused into final sequences to enrich semantic information.

Therefore, we propose a novel Glyph-driven Topology En-

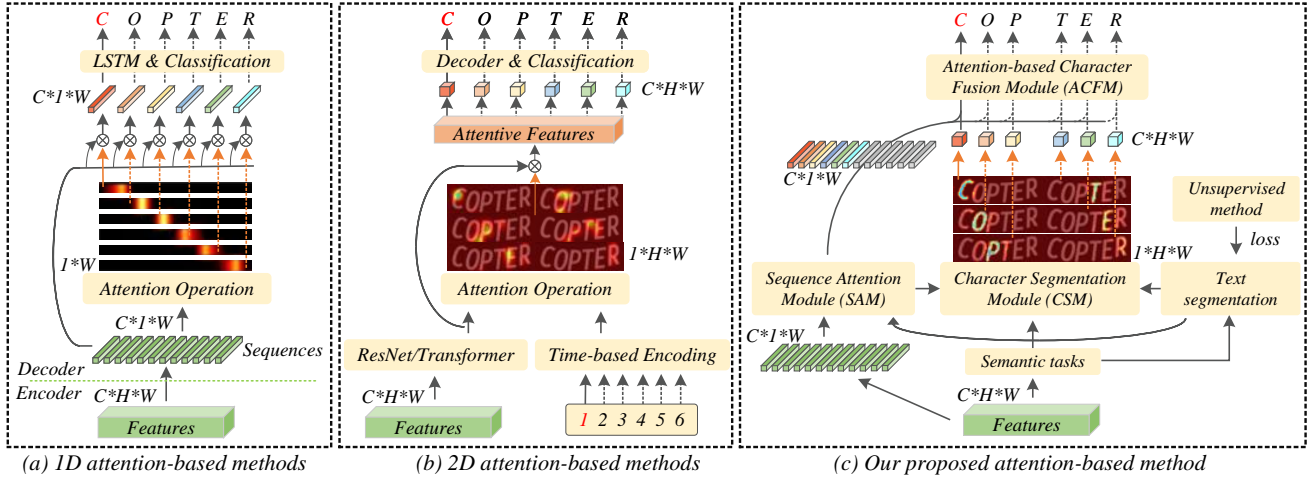


Fig. 1. Comparison of different attention mechanisms in encoder-decoder methods of STR. Text characters in the normalized image are sequentially fed into the encoder and decoder to obtain the predicted characters. The orange dotted line represents the recognition pipeline at future decoding steps. (a) The 1D attention mechanism concentrates on the important items of the encoded sequences. (b) The 2D attention mechanism approximately extracts time-dependent spatial relationships and localizes characters. (c) Our proposed attention mechanism captures and perceives more detailed character topological information without character-level annotations.

hancement Network (GTEN) for STR to address the above-mentioned issues, including alignment-drifted sequential attention and coarse character attention. Specifically, our method contains Sequence Alignment Module (SAM), Character Segmentation Module (CSM), and Attention-based Character Fusion Module (ACFM), as shown in Fig. 1(c). Firstly, in SAM, we address the alignment-drifted sequential attention by establishing constraint functions with 1D learnable attention weights and a text segmentation map optimized by an unsupervised method on text images. Secondly, based on the 1D sequence-aligned attention and the text segmentation map both from SAM, a 2D ordered and multi-channel segmentation result for character classes is generated by the proposed CSM without character-level annotations. It contains more detailed topological information of the glyphs to enrich semantic representations. Finally, an ACFM is designed to integrate more topological features into the 1D attentive contextual features, which frees from the error accumulation raised by the time-dependent decoding manner.

In summary, the main contributions of this paper are three-fold:

- We propose a novel STR model, GTEN, to perceive pixel-wise topological information of the glyphs without extra character-level annotations for scene text recognition. Unlike other coarse character attention, our proposed attention overcomes the bottleneck information acquisition in visual models.
- We establish a SAM to address the alignment drift by building constraint functions to optimize learnable attention weights. Moreover, we construct a CSM by employing the sequence alignment result to generate ordered character segmentation maps with respect to visual features, which provides more topological features. These attentive features are then sequentially fed into a designed

ACFM to generate rich semantic feature representations. To the best of our knowledge, it is the first attempt to utilize an unsupervised method for attention construction on text images.

- Our GTEN achieves competitive performance on scene text datasets and recognizes both regular and irregular texts robustly. Furthermore, experiments demonstrate the effectiveness and potential of unsupervised methods for STR by adding acceptable structural parameters based on TRBA.

## II. RELATED WORKS

Traditional STR methods mainly adopt a bottom-up approach, in which individual character segment is extracted by sliding window [43], [45] and connected components [33]. These detected segments are classified and grouped into text lines to obtain the final recognition result. These methods complicate post-processing steps and rely heavily on the performance of character detectors. Recently, some top-bottom methods have been developed to recognize entire images instead of character segments directly. As shown in a comprehensive survey [4], the type of methods can be divided into four different consecutive stages of operations, *i.e.*, transformation (*Trans.*), feature extraction (*Feat.*), sequence modeling (*Seq.*), and prediction (*Pred.*). However, the main difference lies in the *Trans.* stage and *Seq.* stage.

The goal of rectification-modules in the *Trans.* stage is to adjust irregular images to regular ones by adaptively learning transformation parameters. Specifically, Shi *et al.* [38] first introduce a Spatial Transformer Network (STN) to rectify irregular texts, which utilizes convolutional neural networks (CNNs) to predict a set of fiducial points around the text for thin-plate-spline (TPS) transformation [47]. Zhan *et al.* [52] propose a line fitting transformation that removes text line curvatures. The pose of the text line is estimated by a middle

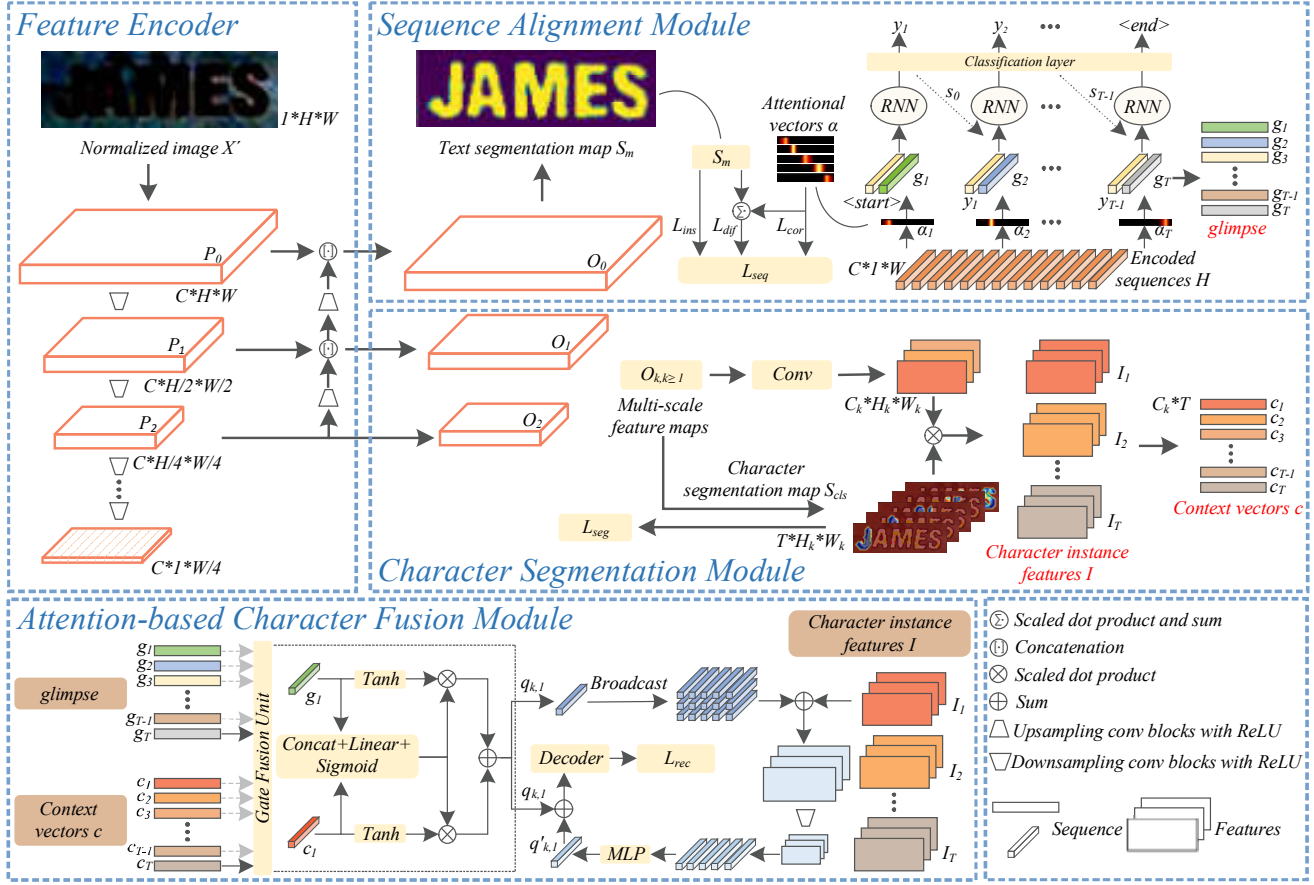


Fig. 2. Details of the glyph-driven topology enhancement network (GTEN). It mainly consists of five parts: image transformation, feature encoder, sequence alignment module, character segmentation module, and attention-based character fusion module.

line and a set of vertical line segments modeled by polynomials. MORAN [28] predicts the horizontal and vertical offsets of each pixel on text images. Without geometric supervision, these transformation parameters of rectification-modules are updated only by the gradients propagated from subsequent recognition networks. Furthermore, to rectify highly curved texts, SCRN [48] constructs geometric representations about text (*i.e.*, center point, scale, character orientation, and text orientation) predicted by CNNs and supervised by character-level labels.

Recent methods capture contextual information in text lines consisting of characters to provide rich semantic features in the *Seq.* stage. For regular text recognition, attention-based methods [7], [9], [26], [37]–[39] execute sequence modeling over a 1D space, where input text images are encoded into a 1D sequential form by CNNs. For example, Shi *et al.* [39] propose a classic encoder-decoder framework to implement sequence-to-sequence learning. It first employs an encoder BiLSTM [12] to capture the long-range dependencies of the input sequence and then outputs its state to the decoder sequentially. For irregular text recognition, compressing curved and distorted text images into 1D sequential features will inevitably bring irrelevant information, generate weak semantic representation, and cause error accumulation. Thus building a 2D attention mechanism

[23], [46], [49] is a mainstream solution. Specifically, Li *et al.* [23] design a tailored 2D attention mechanism that combines feature maps and hidden states of the decoder LSTM [16] to focus on spatial character features at each decoding step. Yu *et al.* [49] obtain attention maps of corresponding characters by expanding the Bahdanau attention mechanism [6] to compute attention scores of all spatial locations of visual features. Lyu *et al.* [29] first employ a fully convolutional network to predict character-level segmentation results, which requires extra character-level annotations, and then perform classification tasks.

### III. METHODOLOGY

#### A. Overall Pipeline

In GTEN, our network mainly consists of five parts: a transformation layer for text image correction, a ResNet backbone [15] for feature extraction, a sequence alignment module for 1D attention generation, two semantic tasks including text segmentation and character segmentation, and an attention-based character fusion module for classification. We illustrate the relationship of our proposed modules of the text recognition network GTEN in Fig. 1(c).

First, the transformation layer employs a Thin Plate Spline (TPS), a variant of the spatial transformation network (STN)

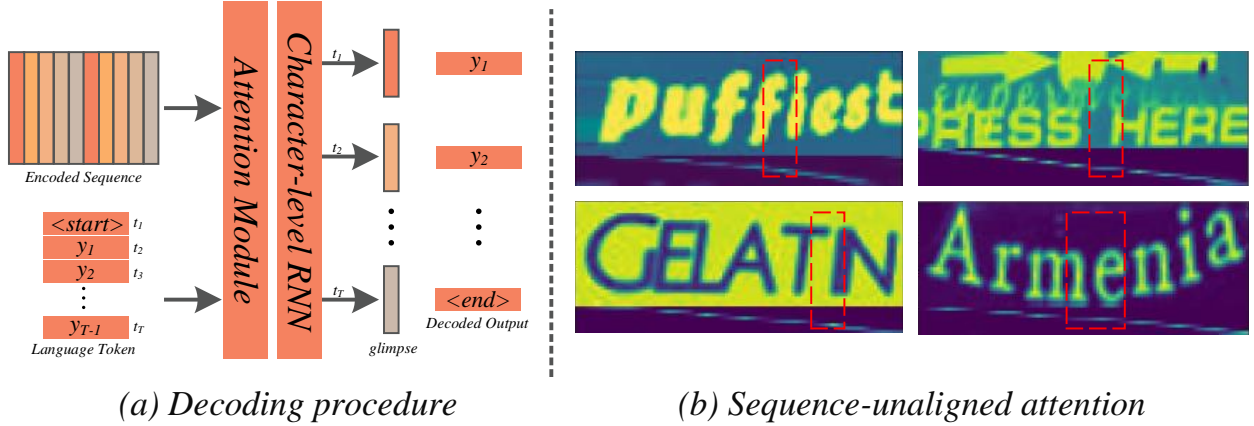


Fig. 3. Illustration of the representative attention-based decoder and some sequence-unaligned attention examples. The red dashed boxes in (b) indicate that the attention weight struggles to align text sequence at the current decoding step.

[18], to transform the cropped text image (*i.e.*, input images  $\mathbf{X}$ ) into a normalized image  $\mathbf{X}'$ . In detail, the TPS transformation utilizes CNNs to predict a predefined number of fiducial points and normalizes the region enclosed by them into a fixed size. Then, the normalized text image are fed into the designed 31-layers ResNet [15] to extract text features. Next, the final output of the backbone is reshaped into a fixed-length sequence (Encoded sequences  $\mathbf{H}$ ) and fed into the SAM to obtain sequence-aligned attention weights ( $\alpha$ , each channel denotes the weight of predefined-length sequences at the current step). And the outputs of *Block 0* and *Block 1* from ResNet are designed to construct channel-wise 2D attention weights ( $\mathbf{S}_{cls}$ , each channel represents an order-specific character segmentation map). Finally, the attentional information (1D and 2D) within text features is fused to predict character classification. We illustrate the specific details of the text recognition network GTEN in Fig. 2.

#### B. Sequence Alignment Module (SAM)

1) *Background*: We first review the representative attention-based STR methods [3], [39], which consists of an encoder and a decoder. The encoder extracts text features  $\mathbf{H} \in \mathbb{R}^{B \times T \times C}$  from the normalized image  $\mathbf{X}'$ , which are then fed into the decoder to predict the character classification. The decoder includes an attentional sequence module, a variant of recurrent neural network (RNN), and a linear layer, as illustrated in Fig. 3(a). Specifically, the text features first are split into  $T$  sequences, and then the sequence ( $\mathbf{h}_t$ ,  $t=\{1,2,3,\dots,T\}$ ) is fed into the recurrent module to generate output vector  $\mathbf{x}_t$  and a new state vector  $\mathbf{s}_t$  at the decoding step  $t$ . The specific details are as follows:

$$(\mathbf{x}_t, \mathbf{s}_t) = \text{rnn}(\mathbf{s}_{t-1}, (\mathbf{g}_t, e(y_{t-1}))), \quad (1)$$

where  $\text{rnn}$  represents a recurrent unit (*e.g.*, LSTM [16], Gate Recurrent Unit (GRU) [10]), and  $(\mathbf{g}_t, e(y_{t-1}))$  denotes the combination of *glimpse*  $\mathbf{g}_t$  and the embedding of the predicted class at the previous decoding step. Especially,  $y_0$  denotes an

artificially defined start token. The *glimpse* is computed by the attention mechanism as follows:

$$\alpha'_{t,i} = \mathbf{w}^T \tanh(\mathbf{W} \mathbf{s}_{t-1} + \mathbf{V} \mathbf{h}_i + b), \quad (2)$$

$$\alpha_{t,i} = \exp(\alpha'_{t,i}) / \sum_{i'=1}^n \exp(\alpha'_{t,i'}), \quad (3)$$

$$\mathbf{g}_t = \sum_{i=1}^n \alpha_{t,i} \mathbf{h}_i, \quad (4)$$

and finally, the output vector predicts the current character classification by a linear layer:

$$p(y_t) = \text{softmax}(\mathbf{W}_o \mathbf{x}_t + b_o), \quad (5)$$

$$y_t \sim p(y_t), \quad (6)$$

where the  $\mathbf{w}, \mathbf{W}, \mathbf{V}, \mathbf{W}_o$  are learnable parameters.

From the formula (1)-(6), the decoding unit obtains the attention weights ( $\alpha_t \in \mathbb{R}^n$ ), indicating the important items of the encoded sequences at decoding step  $t$ , to capture the contextual dependencies between its *glimpse* and last character by recurrent units. Assisted with the implicit language representations, the attention-based STR method effectively recognizes regular text images. However, the positional information drowns as the decoding step increases, which easily leads to alignment drift at latter decoding steps as shown in Fig. 3(b), *i.e.*, the learnable attention weights struggle to align long text sequences [46], [50]. Therefore, we establish constraint functions with the learnable attention weights (1D) and the text segmentation map optimized by an unsupervised method on text images to address the alignment-drifted sequential attention.

2) *Sequence-aligned Attention*: From the background, character information of the encoder outputs highlighted by the attention weights will be fed into the classifier to recognize characters. However, compressing 1D sequential features weighted by the above-mentioned alignment-drifted attention brings incomplete contextual information and causes incorrect recognition. To mitigate the misrecognition results, we propose

an unsupervised segmentation method to alleviate the issue of alignment-drifted attention. Specifically, we first extract the output of *Conv 0*, *Block 0*, and *Block 1* from ResNet, which are defined as  $\mathbf{P}_0$ ,  $\mathbf{P}_1$ , and  $\mathbf{P}_2$ . The bottom-up integration approach is employed as follows:

$$\mathbf{O}_2 = \varphi(\mathbf{P}_2), \quad (7)$$

$$\mathbf{O}_1 = \varphi([\mathcal{T}(\mathbf{O}_2, s_1), \mathbf{P}_1]), \quad (8)$$

$$\mathbf{O}_0 = \varphi([\mathcal{T}(\mathbf{O}_1, s_0), \mathbf{P}_0]), \quad (9)$$

where  $\varphi(\cdot)$  denotes two convolutional layers with BatchNorm and ReLU activation function,  $\mathcal{T}(\cdot)$  refers to single  $2 \times$  up-sampling for  $\mathbf{O}_k$  with resolution  $s_k$  (i.e.,  $H_k * W_k$ ), and  $[\cdot]$  represents the concatenation operation along the channel axis. And then,  $\mathbf{O}_0$  is exploited to produce the final text segmentation mask by a binary classification convolutional layer. To supervise the predicted segmentation results, we adopt a simple K-means clustering method, which does not require additional annotations.

Ideally, if the attention weight vectors are independent of each other, and the sequences they focus on are the ones in which the corresponding character is located, we consider the attention weights generated by the network to be successfully aligned with the set of sequences. Thus, assuming that the text segmentation result is  $\mathbf{S}_m$ , we first sum the correlation coefficient  $S_{\text{cor}}$  between  $L$  attentional vectors, and extract character saliency map  $\mathbf{S}_{\text{sal}}$  by the attentional vectors. The details are as follows:

$$S_{\text{cor}} = \sum_{1 \leq t < t' \leq L} \alpha_t^\top \alpha_{t'}, \quad (10)$$

$$\mathbf{S}_{\text{sal}} = \sum_{t=1}^L (\sigma(\alpha_t) \times \mathbf{S}_m), \quad (11)$$

where  $L$  denotes the character numbers of text images.  $\sigma(\cdot)$  refers to the nonlinear activation function, which uses the variant of sigmoid function to encode the vector mapping to  $[0,1]$ :

$$\sigma(x) = \frac{1}{1 + \exp(-\mu(x - \lambda))}, \quad (12)$$

where  $\mu, \lambda$  are constants, set to 70 and 0.1 in the experiment, respectively. Then the alignment drift problem can be alleviated by minimizing the correlation coefficient  $S_{\text{cor}}$  and the difference  $S_{\text{dif}}$  between  $\mathbf{S}_m$  and  $\mathbf{S}_{\text{sal}}$  in the training stage by the following loss function:

$$\mathcal{L}_{\text{cor}} = S_{\text{cor}}, \quad (13)$$

$$\mathcal{L}_{\text{dif}} = \frac{1}{N} \sum_{i=1}^N -(\rho_i \log(\rho_i^*) + (1 - \rho_i) \log(1 - \rho_i^*)), \quad (14)$$

$$\mathcal{L}_{\text{seq}} = \gamma_1 \mathcal{L}_{\text{ins}} + \gamma_2 \mathcal{L}_{\text{cor}} + \gamma_3 \mathcal{L}_{\text{dif}}, \quad (15)$$

where  $N$  denotes the number of pixels in the text segmentation map  $\mathbf{S}_m$ ,  $\rho_i$  and  $\rho_i^*$  are the confidence score of pixel  $i$  in  $\mathbf{S}_m$  and  $\mathbf{S}_{\text{sal}}$ , respectively.  $\mathcal{L}_{\text{ins}}$  denotes a binary cross-entropy loss between  $\mathbf{S}_m$  and unsupervised results to promote text segmentation performance.

### C. Character Segmentation Module (CSM)

The existing character segmentation methods have the following limitations: 1) Training the segmentation network need to be supervised by character-level annotations, which requires laborious and difficult annotations; 2) The character segmentation maps focus on the character spatial regions while having no detailed topological information of the glyphs; 3) The order of the text characters cannot be directly obtained from the character segmentation maps predicted by deep learning networks.

To address these issues, we propose a supervised segmentation network without extra character-level annotations. It generates ordered and multi-channel segmentation maps for character class by pixel-wise localization. Specifically, followed by a  $1 \times 1$  convolutional layer, the features  $\mathbf{O}_k$  obtained from SAM predict the character segmentation maps  $\mathbf{S}_{\text{cls}}$  with the shape of  $N_s * s_k$ .  $N_s$  is set to  $1 + T$ , including the background and the set maximum length of text characters. Benefit from sequence alignment results, the  $T$  attention vectors  $\alpha_t$  are independent, and the items they focus on from the encoded outputs correspond to the 1D positions where the characters are located. Thus the character ground-truth is generated by the multiplication of attention vector  $\alpha_t$  and the text segmentation mask  $\mathbf{S}_m$  obtained from SAM. Specifically, assuming that the character ground-truth is  $\mathbf{S}_{\text{gt}}$ , we construct it from the concatenation operation as follows:

$$\mathbf{S}_{\text{gt}} = [1 - \mathbf{S}_m, \mathbb{1}_{[\alpha_t > \delta]} \times \mathbf{S}_m], \quad (16)$$

where  $[\cdot]$  represents the concatenation operation along the channel axis.  $\delta$  denotes the confidence threshold, which is set to 0.05 in the experiment. And then, we use the constructed character ground-truth to optimize character segmentation maps by the joint function of multi-class Dice loss [30] and cross-entropy loss, which boosts the segmentation results of the character segmentation maps. We implement the specific details as follows:

$$\mathcal{L}_{\text{dice}} = \frac{1}{L} \sum_{j=2}^{L+1} \left( 1 - \frac{2 \sum_{i=1}^N (\omega_{j,i} \omega_{j,i}^*)}{\sum_{i=1}^N (\omega_{j,i}) + \sum_{i=1}^N (\omega_{j,i}^*)} \right), \quad (17)$$

$$\mathcal{L}_{\text{cel}} = \frac{1}{N} \sum_{i=1}^N -(\rho_i \log(\sum_{j=2}^{T+1} \omega_{j,i}^*) + (1 - \rho_i) \log(1 - \sum_{j=2}^{T+1} \omega_{j,i}^*)), \quad (18)$$

$$\mathcal{L}_{\text{seg}} = \gamma_4 \mathcal{L}_{\text{dice}} + \gamma_5 \mathcal{L}_{\text{cel}}, \quad (19)$$

where  $\omega_{j,i}$  and  $\omega_{j,i}^*$  are the confidence scores of pixel  $i$  of the  $j$ -index map in the ground-truth foreground mask  $\mathbf{S}_{\text{gt}}$  and the character segmentation maps  $\mathbf{S}_{\text{cls}}$ , respectively, and  $\rho_i$  is the confidence score of pixel  $i$  in  $\mathbf{S}_m$ .

Unlike previous methods [11], [23], [46] that embed or model time-dependent sequences to capture 2D attention feature representations of corresponding characters, our method employs 1D sequence-aligned attention to learn multi-channel character segmentation representations from the text segmentation map  $\mathbf{S}_m$ . It promotes the network to perceive and capture more topological information of glyphs supervised by

TABLE I  
THE PARAMETER SETTING TABLE OF GTEN.

Name	Value	Name	Value
Batch size $B$	128	Decoding step $T$	26
Feature channel $C$	256	Sequence length $n$	26
Character length $L$	25	Constant $\lambda, \mu$	0.1, 70
Constant $\gamma_1, \gamma_2, \dots, \gamma_5$	1.0	Constant $S_k$	26
Confidence threshold $\delta$	0.05	Image size $W, H$	100, 32

the additional loss  $\mathcal{L}_{\text{seg}}$ . Moreover, the channel-specific map corresponds to order-specific character attention due to the ordered attention vector  $\alpha_t$ .

#### D. Attention-based Character Fusion Module (ACFM)

As discussed in the SAM and CSM, the visually aligned *glimpse*  $g_t$  and character segmentation maps  $S_{\text{cls}}$  denote two different character feature representations. They belong to different dimensions (*i.e.*, 1D and 2D). Considering that their contributions for STR results should be different among various text images, we dynamically fuse the detailed character segmentation maps and *glimpse* to enrich the semantic information for character recognition. Specifically, the feature map  $O_k \in \mathbb{R}^{W_k \times H_k \times C}$  is first fed into a convolutional layer with BatchNorm and ReLU activation function, and then element-wise multiplied with character segmentation maps  $S_{\text{cls}} \in \mathbb{R}^{W_k \times H_k \times T}$  (remove background) to extract character instance features  $I_k \in \mathbb{R}^{W_k \times H_k \times T \times C}$  with detailed glyph topology information.  $T$  denotes the total decoding steps, and individual character instance features  $I_{k,t} \in \mathbb{R}^{W_k \times H_k \times C}$  are processed at each decoding step.

On the one hand,  $I_{k,t}$  is reshaped into 1D sequence feature  $c_{k,t} \in \mathbb{R}^C$  by average pooling along the channel axis. Inspired by the gate unit [1], the sequence  $c_{k,t}$  and *glimpse*  $g_t$  are dynamically fused at the decoding step  $t$  :

$$z_t = \sigma(\mathbf{W}_z[g_t, c_{k,t}]), \quad (20)$$

$$q_{k,t} = z_t g_t + (1 - z_t) c_{k,t}, \quad (21)$$

where  $\mathbf{W}_z$  is trainable weight.

On the other hand, the *glimpse*  $g_t$  is broadcasted and added with  $I_{k,t}$ , which endows the summed character instance features common implicit linguistic information at each pixel. Then we rescale the summed character features into a fixed size by upsampled or down-sampled operation from resolution  $s_k$  to  $s_2$ . Considering that the fixed-size feature map  $I'_{k,t}$  denotes individual character features at the decoding step  $t$ , we adopt convolutional blocks with kernel height  $H_2$  to extract feature sequences, and then Bahdanau attention [6] is employed to output the weighted character sequence  $q'_{k,t}$ . In formula (1), the recurrent module builds implicit language representations by combining the predicted result from the previous decoding step and the *glimpse*. To enrich semantic feature representations, we embed these 1D final sequences into the decoder by modifying the formula (1) as follows:

$$(\mathbf{x}_{k,t}, s_{k,t}) = \text{rnn}(s_{k,t-1}, (q_{k,t} + q'_{k,t}, e(y_{t-1}))) \quad (22)$$

Finally, the decoder output  $\mathbf{x}_{k,t}$  is fed into a linear layer and a *softmax* operation to output the current decoded classification. Character information interaction and complementarity between multi-scale features further improve text recognition performance by the objective function as follows:

$$\mathcal{L}_{\text{rec}} = -\frac{1}{T} \sum_{k=1}^3 \sum_{t=1}^T \log p(y_t | \mathbf{x}_{k,t}) \quad (23)$$

## IV. EXPERIMENTS

### A. Datasets

Our model is trained on two large-scale synthetic datasets (*i.e.*, SynthText [14], MJSynth [17]). Seven scene text recognition datasets are used to evaluate the performance of our method, including four regular text datasets (*i.e.*, IIIT5K-Words [31], ICDAR2003 [27], ICDAR2013 [20], and Street View Text [44]) and three irregular text datasets (*i.e.*, ICDAR2015 [19], SVT Perspective [34], and CUTE80 [36]). Specifically, the details of these datasets are as follows:

**IIIT5K-Words** (IIIT) [31] contains 5000 images, of which 3000 images for training and 2000 images for evaluation. These text images are cropped from nature scene images and provide ground-truth words.

**Street View Text** (SVT) [44] consists of 257 training images and 647 images for evaluation. These images have low visual contrast, blurry texts, and cluttered backgrounds.

**SVT Perspective** (SP) [34] is similar to SVT that is collected from Google Street View. It contains 645 images for evaluation and many perspective word patches.

**CUTE80** (CT) [36] is constructed for the curved text recognition task, which contains 288 cropped images from the natural scene.

ICDAR series datasets, *i.e.*, ICDAR2003, ICDAR2013, and ICDAR2015, are publicly available<sup>2</sup> for scene text recognition tasks. These datasets are taken from natural scenes, including traffic signs, shopping mall trademarks, billboards, etc. For a fair comparison with many STR manuscripts, we discard some text images whose ground-truth word length is less than three characters or ones that contain non-alphanumeric characters. As a summary in [3], the ICDAR series datasets are used in two different evaluation versions.

**ICDAR2003** (IC03) [27] contains two different versions with 860 and 867 images for evaluation.

**ICDAR2013** (IC13) [20] has 848 training images and 1095 testing images. After selection, 857 and 1,015 images are used for evaluation data, respectively.

**ICDAR2015** (IC15) [19] contains many oriented, curved, and perspective texts, which provides two different versions with 1,811 and 2,077 images for evaluation.

### B. Implementation Details

As a baseline, the code of TRBA model<sup>3</sup> [3] is modified to implement our proposed GTEN on a server with an Nvidia Tesla V100 (32G) GPU in Pytorch<sup>4</sup>. Specifically, we train

<sup>2</sup><https://rrc.cvc.uab.es/>

<sup>3</sup><https://github.com/clovaai/deep-text-recognition-benchmark>

<sup>4</sup><https://pytorch.org/>

TABLE II

COMPARISON RESULTS OF SCENE TEXT RECOGNITION METHODS. ALL METHODS ARE TRAINED ONLY ON TWO LARGE-SCALE SYNTHETIC DATASETS AND EVALUATED ON A JOINT TEST SET OF SEVEN REAL-WORLD BENCHMARKS. MJ AND ST REPRESENT THE MJSYNTH DATASET AND SYNTHTEXT DATASET, RESPECTIVELY. “ABINET-V” DENOTES THE VISION MODEL PROPOSED BY FANG *et al.* [11], AND THE REPORTED RESULT IS IN MMOCR<sup>1</sup>. \* DENOTES IT IS UNCLEAR WHICH VERSION OF THE CURRENT DATASET IS EVALUATED. THE BEST RESULTS IN EACH COLUMN ARE SHOWN IN **BOLD FONT**.

Methods	Train data	IIIT	SVT	IC03		IC13		IC15		SP	CT
		3000	647	860	867	857	1015	1811	2077	645	288
CRNN [37]	MJ	78.2	80.8	89.4	-	-	86.7	-	-	-	-
RARE [38]	MJ	81.9	81.9	90.1	-	88.6	-	-	-	71.8	59.2
ASTER [39]	MJ+ST	93.4	<b>93.6</b>	94.5	-	-	91.8	-	76.1*	78.5	79.5
ScRN [48]	MJ+ST	94.4	88.9	95.0	-	-	93.9	-	78.7	80.8	87.5
MORAN [28]	MJ+ST	91.2	88.3	-	95.0	-	92.4	-	68.8	-	77.4
SAR [23]	MJ+ST	91.5	84.5	-	-	-	91.0	-	69.2	76.4	83.3
TRBA [5]	MJ+ST	92.1	88.9	94.8	95.1	93.9	93.1	78.3	74.7	79.5	78.2
DAN [46]	MJ+ST	94.3	89.2	-	95.0	-	93.9	-	74.5	80.0	84.4
TextScanner [42]	MJ+ST	93.9	90.1	-	-	-	92.9	-	79.4*	84.3	83.3
SE-SAR [35]	MJ+ST	-	85.8	-	-	-	90.9	-	73.4	78.7	-
SRN [49]	MJ+ST	94.8	91.5	-	-	-	<b>95.5</b>	82.7	-	85.1	87.8
PlugNet [32]	MJ+ST	94.4	92.3	95.7	-	-	95.0	-	82.2	84.3	85.0
ViTSTR [2]	MJ+ST	88.4	87.7	94.7	94.3	93.2	92.4	78.5	72.6	81.8	81.3
ABINet-V [11]	MJ+ST	94.7	91.7	-	-	-	93.6	-	<b>83.0</b>	<b>85.1</b>	86.5
GTEN (ours)	MJ+ST	<b>95.4</b>	91.2	<b>96.0</b>	<b>95.4</b>	<b>96.9</b>	95.0	<b>82.9</b>	80.1	84.4	<b>89.9</b>

TABLE III

COMPARISON RESULTS OF SCENE TEXT RECOGNITION METHODS USING REAL-WORLD DATA. “R” DENOTES THE COLLECTION OF TRAINING SETS OF REAL LABELED DATASETS.

Methods	Train data	IIIT	SVT	IC03		IC13		IC15		SP
		3000	647	860	867	857	1015	1811	2077	645
SAR [23]	MJ+ST+R	95.0	91.2	-	-	-	94.0	-	78.8	<b>86.4</b>
TextScanner [42]	MJ+ST+R	95.7	<b>92.7</b>	-	-	-	94.9	83.5	-	84.8
RobustScanner [50]	MJ+ST+R	95.1	89.2	-	-	-	93.1	-	77.8	80.3
GTEN+real (ours)	MJ+ST+R	<b>96.0</b>	92.4	<b>95.8</b>	<b>95.6</b>	<b>96.6</b>	<b>95.2</b>	<b>84.3</b>	<b>80.9</b>	84.6

our model by the combination of Adam optimizer [21] and AdaDelta Optimizer [51]. We adopt the Adam optimizer and the one-cycle learning rate scheduler [40] with a maximum learning rate of 0.0005 to train the ResNet backbone. Also, the remaining modules are trained by the AdaDelta optimizer with a decay rate of 0.95 and the multi-step learning rate scheduler with the initial learning rate of 1.0. Gradient clipping of all trainable parameters is set at a magnitude of 5. In the experiment, the parameter details are shown in Table I. To fairly compare with other visual-based methods, validating and evaluating details are the same as [3].

### C. Comparison with State of the Art

We compare with the state-of-the-art methods [2], [5], [11], [23], [28], [32], [35], [37]–[39], [42], [46], [48], [49] to evaluate the effectiveness of our method. These methods propose various 1D or 2D attention mechanisms to focus on character features, which are fed into the decoder to output character categories. As shown in Table II, our method achieves the best results on the IIIT, ICDAR-series and CT datasets by modifying on top of the simple TRBA module, which demonstrates that excavating the topology features of characters is essential to improve the performance of vision models. Unlike most 2D attention mechanisms that approximately extract spatial

relationships by the time-dependent decoding manner, GTEN perceives more detailed topological information of the glyphs assisted by a simple unsupervised method, which further indicates the effectiveness and potential of our proposed method for STR tasks. Moreover, topology features with more detailed visual information are fed into the decoder in the right order, which enriches semantic representations and frees from the error accumulation raised by only sequence-based models. Our attention visualization results are shown in Fig. 4.

Compared to training the scene text recognition network using only synthetic datasets, real-world data in the same domain as the evaluation data can facilitate the network to converge quickly to the target domain. To demonstrate the potential of our proposed method, we add the training set of real-world datasets, including IIIT, SVT, IC13, IC15, and COCO [41], to train our method. As shown in Table III, the “GTEN+real” method achieves competitive performance compared to the reported results of other scene text recognition methods evaluated on real-world datasets, especially getting a significant performance improvement on the IC15 test set, which demonstrates the feasibility and effectiveness of our method training on real data.

<sup>4</sup><https://github.com/open-mmlab/mmocr>



Fig. 4. Visualization examples of our proposed 2D attention mechanism generated by GTEN. The left side of each example is the original text image, and the right side is the heat map constructed from the normalized text image and character segmentation maps generated by CSM. More visualization results are provided in the supplementary material.

TABLE IV

ABLATION STUDY OF THE PROPOSED GTEN STRUCTURE. WE USE THE “TRBA-BASELINE-SYNTH” MODEL PROPOSED IN [3] AS BASELINE. “JS” MEANS THE JOINT STRUCTURE OF SAM AND CSM. THEY ARE EVALUATED AS A WHOLE STRUCTURE DUE TO THEIR INTERDEPENDENCE. “MS” STANDS FOR MULTI-SCALE TRAINING. THE AVERAGE COLUMN IS THE ARITHMETIC MEAN RESULT OF ALL BENCHMARK DATASETS BY SIZE.

Method	IIIT 3000	SVT 647	IC03		IC13		IC15		SP 645	CT 288	Average
Baseline (TRBA)	92.1	88.9	94.8	95.1	93.9	93.1	78.3	74.7	79.5	78.2	86.48
Baseline+JS	94.8	89.8	94.8	94.7	96.2	94.4	81.5	78.1	82.0	88.9	88.90
Baseline+JS+MS	95.2	90.6	95.5	95.1	96.4	94.5	82.8	79.6	84.3	89.5	89.73
Baseline+JS+MS+ACFM	95.4	91.2	96.0	95.4	96.9	95.0	82.9	80.1	84.4	89.9	90.06

#### D. Ablation Study

1) *Hyper-parameters*: We adjust the parameter of SAM and CSM by performing the joint structure of SAM and CSM. We first set confidence threshold  $\delta$  to 0.05, 0.1, and 0.15, respectively, which the average accuracy on seven benchmarks is 89.73%, 89.27% and 88.73%. By observing the attention weight values generated by the SAM module, we then choose three suitable activation function variants with parameter  $\lambda$  of 0.05, 0.1, and 0.15, and parameter  $\mu$  of 100, 70, and 40, respectively, to encode the weight values to  $[0, 1]$ . Consequently, the average accuracy on seven benchmarks is 89.47%, 89.75% and 89.73%, respectively. Thus, the best parameter is adopted in GTEN as default.

2) *Network Structure*: Our GTEN architecture changes are implemented based on the TRBA. A joint structure of SAM and CSM is added to extract detailed character topology information. And then, it is multiplied with the encoded feature maps to obtain multi-scale character instance features, which are fused with semantic features to improve the recognition results in ACFM. Considering that the character segmentation maps generated by CSM are based on the 1D sequence-aligned attention and text segmentation map from SAM, thus we perform the “Baseline+JS” model with our designed joint structure JS to evaluate the effectiveness of our structure. As depicted in Table IV, the “Baseline+JS” model outperforms the accuracy of the TRBA model on most benchmark datasets, including IIIT, SVT, IC13, IC15, SP and CT. Despite its

simplicity and adding few parameters (from  $49.6 \times 10^6$  to  $59.6 \times 10^6$ ) on the basis of TRBA, the “Baseline+JS” achieves performance gains by a large margin (2.42%) in the average accuracy compared with the TRBA model, which indicates that the attentive character features extracted by the JS structure are effective and important to facilitate character recognition. Our attention mechanism captures pixel-wise topological information of the glyphs, which effectively promotes the network to learn rich feature representations. Moreover, character information interaction and complementarity between multi-scale features further improve text recognition performance by 0.83%. Finally, the gain of adding ACFM is improved by 0.33% from 89.73% to 90.06% in the average accuracy metric.

#### V. CONCLUSIONS

In this paper, we proposed an end-to-end Glyph-driven Topology Enhancement Network (GTEN) for scene text recognition. The proposed method alleviates the issues of alignment drift and coarse character attention by designing the Sequence Alignment Module (SAM), Character Segmentation Module (CSM), and Attention-based Character Fusion Module(ACFM). SAM employs an unsupervised method to optimize the attention drift problem. Benefiting from the sequence alignment results, CSM generates ordered and multi-channel segmentation maps for character class by pixel-wise localization, which contains more detailed topological information of the glyphs rather than coarse attention raised by the time-

dependent decoding manner. More effective visual features are then fused to promote GTEN bring performance improvement. Finally, our GTEN achieves the best performance on public available scene text datasets.

## REFERENCES

- [1] Arevalo, J., Solorio, T., Montes-y Gómez, M., González, F.A.: Gated multimodal units for information fusion. arXiv preprint arXiv:1702.01992 (2017)
- [2] Atienza, R.: Vision transformer for fast and efficient scene text recognition. arXiv preprint arXiv:2105.08582 (2021)
- [3] Baek, J., Kim, G., Lee, J., Park, S., Han, D., Yun, S., Oh, S.J., Lee, H.: What is wrong with scene text recognition model comparisons? dataset and model analysis. In: Proceedings of the IEEE/CVF International Conference on Computer Vision (ICCV). pp. 4715–4723 (2019)
- [4] Baek, J., Kim, G., Lee, J., Park, S., Han, D., Yun, S., Oh, S.J., Lee, H.: What is wrong with scene text recognition model comparisons? dataset and model analysis. In: Proceedings of the IEEE/CVF International Conference on Computer Vision (ICCV). pp. 4715–4723 (2019)
- [5] Baek, J., Matsui, Y., Aizawa, K.: What if we only use real datasets for scene text recognition? toward scene text recognition with fewer labels. In: Proceedings of the IEEE/CVF Conference on Computer Vision and Pattern Recognition (CVPR). pp. 3113–3122 (2021)
- [6] Bahdanau, D., Cho, K., Bengio, Y.: Neural machine translation by jointly learning to align and translate. arXiv preprint arXiv:1409.0473 (2014)
- [7] Bai, F., Cheng, Z., Niu, Y., Pu, S., Zhou, S.: Edit probability for scene text recognition. In: Proceedings of the IEEE/CVF Conference on Computer Vision and Pattern Recognition (CVPR). pp. 1508–1516 (2018)
- [8] Biten, A.F., Tito, R., Mafla, A., Gomez, L., Rusinol, M., Valveny, E., Jawahar, C., Karatzas, D.: Scene text visual question answering. In: Proceedings of the IEEE/CVF international conference on computer vision. pp. 4291–4301 (2019)
- [9] Cheng, Z., Bai, F., Xu, Y., Zheng, G., Pu, S., Zhou, S.: Focusing attention: Towards accurate text recognition in natural images. In: Proceedings of the IEEE/CVF International Conference on Computer Vision (ICCV). pp. 5076–5084 (2017)
- [10] Cho, K., Van Merriënboer, B., Gulcehre, C., Bahdanau, D., Bougares, F., Schwenk, H., Bengio, Y.: Learning phrase representations using rnn encoder-decoder for statistical machine translation. arXiv preprint arXiv:1406.1078 (2014)
- [11] Fang, S., Xie, H., Wang, Y., Mao, Z., Zhang, Y.: Read like humans: Autonomous, bidirectional and iterative language modeling for scene text recognition. In: Proceedings of the IEEE/CVF Conference on Computer Vision and Pattern Recognition (CVPR). pp. 7098–7107 (2021)
- [12] Graves, A., Liwicki, M., Fernández, S., Bertolami, R., Bunke, H., Schmidhuber, J.: A novel connectionist system for unconstrained handwriting recognition. IEEE Transactions on Pattern Analysis and Machine Intelligence (TPAMI) **31**(5), 855–868 (2008)
- [13] Guan, T., Gu, C., Lu, C., Tu, J., Feng, Q., Wu, K., Guan, X.: Industrial scene text detection with refined feature-attentive network. IEEE Transactions on Circuits and Systems for Video Technology (TCSVT) (2022)
- [14] Gupta, A., Vedaldi, A., Zisserman, A.: Synthetic data for text localisation in natural images. In: Proceedings of the IEEE/CVF Conference on Computer Vision and Pattern Recognition (CVPR). pp. 2315–2324 (2016)
- [15] He, K., Zhang, X., Ren, S., Sun, J.: Deep residual learning for image recognition. In: Proceedings of the IEEE/CVF Conference on Computer Vision and Pattern Recognition (CVPR). pp. 770–778 (2016)
- [16] Hochreiter, S., Schmidhuber, J.: Long short-term memory. Neural computation **9**(8), 1735–1780 (1997)
- [17] Jaderberg, M., Simonyan, K., Vedaldi, A., Zisserman, A.: Synthetic data and artificial neural networks for natural scene text recognition. arXiv preprint arXiv:1406.2227 (2014)
- [18] Jaderberg, M., Simonyan, K., Zisserman, A., et al.: Spatial transformer networks. Advances in Neural Information Processing Systems **28**, 2017–2025 (2015)
- [19] Karatzas, D., Gomez-Bigorda, L., Nicolaou, A., Ghosh, S., Bagdanov, A., Iwamura, M., Matas, J., Neumann, L., Chandrasekhar, V.R., Lu, S., et al.: Icdar 2015 competition on robust reading. In: Proceedings of the International Conference on Document Analysis and Recognition (ICDAR). pp. 1156–1160. IEEE (2015)
- [20] Karatzas, D., Shafait, F., Uchida, S., Iwamura, M., i Bigorda, L.G., Mestre, S.R., Mas, J., Mota, D.F., Almazan, J.A., De Las Heras, L.P.: Icdar 2013 robust reading competition. In: Proceedings of the International Conference on Document Analysis and Recognition (ICDAR). pp. 1484–1493. IEEE (2013)
- [21] Kingma, D.P., Ba, J.: Adam: A method for stochastic optimization. arXiv preprint arXiv:1412.6980 (2014)
- [22] Lee, J., Park, S., Baek, J., Oh, S.J., Kim, S., Lee, H.: On recognizing texts of arbitrary shapes with 2d self-attention. In: Proceedings of the IEEE/CVF Conference on Computer Vision and Pattern Recognition Workshops. pp. 546–547 (2020)
- [23] Li, H., Wang, P., Shen, C., Zhang, G.: Show, attend and read: A simple and strong baseline for irregular text recognition. In: Proceedings of the AAAI Conference on Artificial Intelligence (AAAI). pp. 8610–8617 (2019)
- [24] Liao, M., Zhang, J., Wan, Z., Xie, F., Liang, J., Lyu, P., Yao, C., Bai, X.: Scene text recognition from two-dimensional perspective. In: Proceedings of the AAAI Conference on Artificial Intelligence (AAAI). pp. 8714–8721 (2019)
- [25] Litman, R., Anschel, O., Tsiper, S., Litman, R., Mazor, S., Manmatha, R.: Scatter: selective context attentional scene text recognizer. In: Proceedings of the IEEE/CVF Conference on Computer Vision and Pattern Recognition (CVPR). pp. 11962–11972 (2020)
- [26] Liu, Z., Li, Y., Ren, F., Goh, W.L., Yu, H.: Squeezedtext: A real-time scene text recognition by binary convolutional encoder-decoder network. In: Proceedings of the AAAI Conference on Artificial Intelligence (AAAI) (2018)
- [27] Lucas, S.M., Panaretos, A., Sosa, L., Tang, A., Wong, S., Young, R., Ashida, K., Nagai, H., Okamoto, M., Yamamoto, H., et al.: Icdar 2003 robust reading competitions: entries, results, and future directions. International Journal of Document Analysis and Recognition (IJDAR) **7**(2-3), 105–122 (2005)
- [28] Luo, C., Jin, L., Sun, Z.: Moran: A multi-object rectified attention network for scene text recognition. Pattern Recognition (PR) **90**, 109–118 (2019)
- [29] Lyu, P., Liao, M., Yao, C., Wu, W., Bai, X.: Mask textspotter: An end-to-end trainable neural network for spotting text with arbitrary shapes. In: Proceedings of the European Conference on Computer Vision (ECCV). pp. 67–83 (2018)
- [30] Milletari, F., Navab, N., Ahmadi, S.A.: V-net: Fully convolutional neural networks for volumetric medical image segmentation. In: 2016 fourth international conference on 3D vision (3DV). pp. 565–571. IEEE (2016)
- [31] Mishra, A., Alahari, K., Jawahar, C.: Scene text recognition using higher order language priors. In: BMVC-British Machine Vision Conference. BMVA (2012)
- [32] Mou, Y., Tan, L., Yang, H., Chen, J., Liu, L., Yan, R., Huang, Y.: Plugnet: Degradation aware scene text recognition supervised by a pluggable super-resolution unit. In: Proceedings of the European Conference on Computer Vision (ECCV). pp. 158–174. Springer (2020)
- [33] Neumann, L., Matas, J.: Real-time scene text localization and recognition. In: Proceedings of the IEEE/CVF Conference on Computer Vision and Pattern Recognition (CVPR). pp. 3538–3545. IEEE (2012)
- [34] Phan, T.Q., Shivakumara, P., Tian, S., Tan, C.L.: Recognizing text with perspective distortion in natural scenes. In: Proceedings of the IEEE International Conference on Computer Vision (ICCV). pp. 569–576 (2013)
- [35] Qiao, Z., Zhou, Y., Yang, D., Zhou, Y., Wang, W.: Seed: Semantics enhanced encoder-decoder framework for scene text recognition. In: arXiv (2020)
- [36] Risnumawan, A., Shivakumara, P., Chan, C.S., Tan, C.L.: A robust arbitrary text detection system for natural scene images. Expert Systems with Applications **41**(18), 8027–8048 (2014)
- [37] Shi, B., Bai, X., Yao, C.: An end-to-end trainable neural network for image-based sequence recognition and its application to scene text recognition. IEEE Transactions on Pattern Analysis and Machine Intelligence (TPAMI) **39**(11), 2298–2304 (2016)
- [38] Shi, B., Wang, X., Lyu, P., Yao, C., Bai, X.: Robust scene text recognition with automatic rectification. In: Proceedings of the IEEE/CVF

Conference on Computer Vision and Pattern Recognition (CVPR). pp. 4168–4176 (2016)

[39] Shi, B., Yang, M., Wang, X., Lyu, P., Yao, C., Bai, X.: Aster: An attentional scene text recognizer with flexible rectification. *IEEE Transactions on Pattern Analysis and Machine Intelligence (TPAMI)* **41**(9), 2035–2048 (2018)

[40] Smith, L.N., Topin, N.: Super-convergence: Very fast training of neural networks using large learning rates. In: Artificial intelligence and machine learning for multi-domain operations applications. vol. 11006, p. 1100612. International Society for Optics and Photonics (2019)

[41] Veit, A., Matera, T., Neumann, L., Matas, J., Belongie, S.: Coco-text: Dataset and benchmark for text detection and recognition in natural images. *arXiv preprint arXiv:1601.07140* (2016)

[42] Wan, Z., He, M., Chen, H., Bai, X., Yao, C.: Textscanner: Reading characters in order for robust scene text recognition. In: Proceedings of the AAAI Conference on Artificial Intelligence (AAAI). pp. 12120–12127 (2020)

[43] Wang, K., Babenko, B., Belongie, S.: End-to-end scene text recognition. In: Proceedings of the IEEE/CVF International Conference on Computer Vision (ICCV). pp. 1457–1464. IEEE (2011)

[44] Wang, K., Babenko, B., Belongie, S.: End-to-end scene text recognition. In: Proceedings of the IEEE/CVF International Conference on Computer Vision (ICCV). pp. 1457–1464. IEEE (2011)

[45] Wang, K., Belongie, S.: Word spotting in the wild. In: Proceedings of the European Conference on Computer Vision (ECCV). pp. 591–604. Springer (2010)

[46] Wang, T., Zhu, Y., Jin, L., Luo, C., Chen, X., Wu, Y., Wang, Q., Cai, M.: Decoupled attention network for text recognition. In: Proceedings of the AAAI Conference on Artificial Intelligence (AAAI). pp. 12216–12224 (2020)

[47] Warps, F.L.B.P.: Thin-plate splines and the decompositions of deformations. *IEEE Transactions on Pattern Analysis and Machine Intelligence (TPAMI)* **11**(6) (1989)

[48] Yang, M., Guan, Y., Liao, M., He, X., Bian, K., Bai, S., Yao, C., Bai, X.: Symmetry-constrained rectification network for scene text recognition. In: Proceedings of the IEEE/CVF International Conference on Computer Vision (ICCV). pp. 9147–9156 (2019)

[49] Yu, D., Li, X., Zhang, C., Liu, T., Han, J., Liu, J., Ding, E.: Towards accurate scene text recognition with semantic reasoning networks. In: Proceedings of the IEEE/CVF Conference on Computer Vision and Pattern Recognition (CVPR). pp. 12113–12122 (2020)

[50] Yue, X., Kuang, Z., Lin, C., Sun, H., Zhang, W.: Robustscanner: Dynamically enhancing positional clues for robust text recognition. In: Proceedings of the European Conference on Computer Vision (ECCV). pp. 135–151. Springer (2020)

[51] Zeiler, M.D.: Adadelta: an adaptive learning rate method. *arXiv preprint arXiv:1212.5701* (2012)

[52] Zhan, F., Lu, S.: Esir: End-to-end scene text recognition via iterative image rectification. In: Proceedings of the IEEE/CVF Conference on Computer Vision and Pattern Recognition (CVPR). pp. 2059–2068 (2019)